

LA-11239-MS

01

*Numerical Modeling of
the Effect of Particle Size of
Explosives on Shock Initiation Properties*

For Reference

Not to be taken from this room

LOS ALAMOS NATL LAB LIBS.



3 9338 00115 9994

Los Alamos

*Los Alamos National Laboratory is operated by the University of California for
the United States Department of Energy under contract W-7405-ENG-36.*

Edited by Sharon Crane, Group M-8

An Affirmative Action/Equal Opportunity Employer

This report was prepared as an account of work sponsored by an agency of the United States Government. Neither the United States Government nor any agency thereof, nor any of their employees, makes any warranty, express or implied, or assumes any legal liability or responsibility for the accuracy, completeness, or usefulness of any information, apparatus, product, or process disclosed, or represents that its use would not infringe privately owned rights. Reference herein to any specific commercial product, process, or service by trade name, trademark, manufacturer, or otherwise, does not necessarily constitute or imply its endorsement, recommendation, or favoring by the United States Government or any agency thereof. The views and opinions of authors expressed herein do not necessarily state or reflect those of the United States Government or any agency thereof.

*Numerical Modeling of
the Effect of Particle Size of
Explosives on Shock Initiation Properties*

*Charles L. Mader
James D. Kershner*



NUMERICAL MODELING OF THE EFFECT OF PARTICLE SIZE OF EXPLOSIVES ON SHOCK INITIATION PROPERTIES

by

Charles L. Mader and James D. Kershner

ABSTRACT

The three-dimensional Eulerian reactive hydrodynamic code 3DE has been used to investigate the effects of particle size and the resulting void or hole size on the shock initiation of heterogeneous explosive charges of TNT. Shocks interacting with TNT containing various hole sizes have been modeled. The void fraction was held at 0.5% while the spherical hole sizes were varied from 0.5- to 0.0005-mm radius, and the TNT was shocked to 12.5 GPa. As the hole size was varied from 0.5 to 0.05 mm, the explosive became more sensitive to shock as the hole size decreased, and the number of hot spots increased. When the hole size was decreased to 0.0005 mm, a 12.5-GPa shock wave failed to build toward propagating detonation because the resulting hot spots were cooled by side rarefactions before appreciable decomposition occurred. At the same density, the most shock-sensitive explosive will be that with particle sizes between coarse and extremely fine material.

I. INTRODUCTION

The effects of particle size and the resulting hole or void size on the shock initiation properties of cast and pressed heterogeneous explosives have been studied using the wedge test and the gap test for many years. Cast TNT has been observed to be less shock sensitive than pressed TNT at the same density. Cast TNT has fewer and larger holes than pressed TNT, resulting in fewer hot spots that are too

far apart to be as effective in supporting the reactive shock wave as pressed charges with more, although smaller, hot spots. Campbell, Davis, Ramsay, and Travis (1) have used the wedge test to measure the distance of run to detonation as a function of shock pressure (the Pop plot) for pressed-TNT charges of coarse TNT (200-250 micrometer) and found that they are less shock sensitive than pressed charges of finer TNT (20-25 micrometers).

Donna Price (2) has reviewed the effect of particle size on the shock sensitivity of pure porous explosives considering both gap test and wedge test data. She showed that in many gap tests, coarse porous explosive seems more shock sensitive than fine, whereas in most wedge tests, the reverse is true. She concludes that the apparent reversal is actually a result of crossing Pop plots and that the gap tests sense a lower pressure region than that usually available in wedge test data.

Moulard, Kury, and Delclos (3) studied two special monomodal RDX/polyurethane cast-PBX formulations of 70 wt% RDX (either 6-micrometer or 134-micrometer median particle size) and 30 wt% polyurethane. The shock initiation properties of these formulations were measured in thin-plate impact, projectile impact, and wedge tests. The formulations containing the fine RDX were significantly less sensitive than that with coarse RDX at the same density of 1.44 g/cm^3 , at least up to 10.0-GPa shock pressure. From these studies, we conclude that at the same density, the most shock-sensitive explosives are those with particle sizes between the coarse particles and the very fine particles.

Heterogeneous explosives are initiated and may propagate by the process of shock interaction with density discontinuities such as voids. These interactions result in hot regions that decompose and produce increasing pressures causing more and hotter decomposition regions. The shock wave increases in strength, releasing more and more energy, until it becomes strong enough that all the explosive reacts and detonation begins. This process is described by the "hydrodynamic hot-spot" model, which models the hot-spot formation from the shock interactions that occur at density discontinuities and describes the decomposition using the Arrhenius rate law and the temperature from the HOM equation of state (4).

The numerical modeling of the interaction of a shock wave with a single density discontinuity was reported in Ref. (4), where an 8.5-GPa shock interacting with a single spherical hole in nitromethane was studied. The study was extended to four

rectangular holes (4). It was determined that 0.0032-mm-radius cylindrical voids would build toward detonation and 0.001-mm-radius voids would form hot spots that failed to propagate because of rarefactions cooling the reactive wave.

The process of shock initiation of heterogeneous explosives has been analyzed (5) numerically by studying the interaction of shock waves with a cube of nitromethane containing 91 holes. An 8.5-GPa shock interacting with a single 0.002-mm hole did not build toward detonation. When the shock wave interacted with a matrix of 0.002-mm holes, it became strong enough to build toward detonation. When the size of the holes was reduced to 0.0004 mm, a marginal amount of the explosive decomposed to compensate for the energy loss to the flow caused by the shock wave interacting with the holes. The shock wave slowly grew stronger, but it did not build to detonation in the time of the calculation.

A 5.5-GPa shock wave interacting with a matrix of 0.002-mm holes resulted in insufficient heating of the resulting hot spots to cause significant decomposition. Desensitization by preshocking resulted when holes were closed by the low-pressure initial 5.5-GPa shock wave. A higher pressure (8.5-GPa) shock wave that arrived later had no holes with which to interact and behaved like a shock wave in a homogeneous explosive until it caught up with the lower pressure preshock wave.

The interaction of a shock wave with a single air hole and a matrix of air holes in PETN, HMX, and TATB was modeled in Ref. (6). The basic differences between shock-sensitive explosives (PETN or HMX) and shock-insensitive explosives (TATB or nitroguanidine) were described by the hydrodynamic hot-spot model. The desensitization of TATB and resulting quenching of a propagating detonation were also modeled using the hydrodynamic hot-spot model.

The hydrodynamic hot-spot model has been used to model the basic processes in the shock initiation of heterogeneous explosives. Interaction of a shock wave with density discontinuities, the resulting hot-spot formation, interaction, and the buildup toward detonation or failure have been modeled. The hydrodynamic hot-spot model has been used to investigate the basic differences between shock-sensitive and shock-insensitive explosives. The hydrodynamic hot-spot model has been used to model the basic processes that occur when a heterogeneous explosive has been shocked with a pressure too low to cause propagating detonation in the time of interest. The explosive is desensitized by the preshock, and a propagating

detonation wave can be quenched when the detonation front arrives at the previously shocked explosive.

From the hydrodynamic hot-spot model (4-6), we can postulate that the coarse-particle explosives have fewer holes or voids per unit volume than the fine-particle explosives, resulting in fewer but larger hot spots. As the explosive particles become finer, the number of hot spots formed by a shock wave increases while the hot spot size decreases. When the explosive becomes very fine, the hot-spot size can become so small that the hot spots cool from side rarefactions before appreciable decomposition can occur. This results in a less shock-sensitive explosive if the explosive has very fine particle sizes. In this paper, we will describe a three-dimensional study of the effect of particle size and the resulting void or hole size on the shock initiation of heterogeneous charges of TNT using the three-dimensional hydrodynamic hot-spot model for shock initiation of heterogeneous explosives.

II. NUMERICAL MODELING

The three-dimensional Eulerian reactive hydrodynamic code 3DE is described in detail in Ref. (7). It uses techniques identical to those described in detail in Ref. (4) and used successfully for describing two-dimensional Eulerian flow with mixed cells and multicomponent equations of state and for modeling reactive flow. It has been used to study the interaction of multiple detonation waves (8), the basic processes of shock initiation of heterogeneous explosives (4-6), the reactive hydrodynamics of a matrix of tungsten particles in HMX (9), and the reaction zone in heterogeneous explosives (10).

The Arrhenius reactive rate law was used with the constants determined experimentally by Raymond N. Rogers and described in Ref. (4). The TNT Arrhenius activation energy used was 34.4 kcal/mole and the frequency factor used was $2.51 \times 10^5 \mu\text{s}^{-1}$.

The HOM equation-of-state constants used for TNT detonation products were the BKW equation-of-state constants given in Ref. (11). The nonreactive solid HOM equation-of-state constants used are given in Table 1 and the Hugoniot states are given in Table 2.

TABLE 1
HOM Solid Constants for Nonreactive TNT
at 1.64 g/cm³

C	+2.2000000000E-01
S	+1.7660000000E+00
F _s	-2.71235359951E+00
G _s	-4.86625796696E+01
H _s	-1.02215618376E+02
I _s	-9.01182904938E+01
J _s	-2.60329744463E+01
γ	+1.5000000000E+00
C _v	+2.9300000000E-01
V _o	+6.09756097561E-01
α	+5.0000000000E-05

A constant velocity piston was applied to the bottom of the explosive cube, shocking the explosive initially to the desired pressure. When the shock wave interacts with a hole, a hot spot with temperatures several hundred degrees hotter than the surrounding explosive is formed in the region above the hole when it is collapsed by the shock wave. The hot region decomposes and contributes energy to the shock wave, which has been degraded by the hole interaction. Whether this energy is sufficient to compensate for the loss from the hole interaction depends on the magnitude of the initial shock wave, the hole size, and the interaction with the flow from its nearest neighbor hot spots.

Shocks interacting with TNT of various particle sizes have been modeled. The effects of a 15.0- and a 12.5-GPa shock on single air holes in TNT have been modeled. The effect of a 12.5-GPa shock wave on a matrix of spherical air holes in TNT has been modeled with the void fraction held at 0.5% and the hole size varied from 0.5- to 0.0005-mm radius. Calculations were performed using 22 by 29 by 111 or 70,818 cells with a particle diameter of at least two cells. The spherical air holes were placed on a hexagonal close-packed lattice. Five layers of cells above the piston did

not contain any holes. With 2 cells per sphere diameter, the matrix contains 72 holes.

The interaction of a 15.0-GPa shock wave in TNT with a single spherical air hole of 0.5-mm radius is shown in Fig. 1. It builds toward a detonation. The interaction of a 12.5-GPa shock wave in TNT with a single spherical air hole of 0.5-mm radius is shown in Fig. 2. It is marginally failing to build to detonation. The interaction of a 15.0-GPa shock wave in TNT with a single spherical air hole of 0.05-mm radius is shown in Fig. 3. It is failing to build to detonation. Increased shock pressure results in larger hot spots that decompose more of the explosive and result in increased sensitivity of the explosive to shock, while smaller holes result in decreased sensitivity.

Although a single 0.5-mm- or a 0.05-mm-radius hole shocked to 12.5 GPa fails to build toward a detonation, a matrix of holes with a void fraction of 0.5% (density of 1.6318 g/cm^3) builds toward detonation, as shown in Figs. 4 and 5. The matrix of 0.05-mm holes builds more quickly than the matrix of 0.5-mm holes. The increased number of holes results in more hot spots that decompose the explosive and increase the sensitivity of the explosive to shock.

A matrix of 0.0005-mm holes shocked to 12.5 GPa fails to result in appreciable explosive decomposition, and the flow fails to build to detonation, as shown in Fig. 6. The hole size is so small that the resulting hot spot is cooled by side rarefactions before appreciable decomposition can occur.

As the hole size was varied from 0.5 to 0.05 mm, the explosive became more sensitive to shock as the hole size decreased, and the number of holes and resulting hot spots increased. Decreasing the hole size to 0.0005 mm resulted in hot spots that were cooled by side rarefactions before appreciable decomposition occurred. At the same density, the most shock-sensitive explosive was the one with 0.05-mm holes. The numerical examples demonstrate that the most shock-sensitive explosive is that with particle sizes between coarse and extremely fine particle sizes.

Decreasing the hole size while holding the density constant results in more holes of smaller size. The most shock-sensitive matrix is the one with 0.05-mm-radius holes, corresponding to a fine-particle explosive. The less sensitive matrix consisting of 0.5-mm-radius holes corresponds to a coarse-particle explosive. The matrix with 0.0005-mm-radius holes is the least shock-sensitive matrix and corresponds to an explosive of very fine particle size.

III. CONCLUSIONS

The three-dimensional Eulerian reactive hydrodynamic code 3DE has been used to investigate the effect of particle size and the resulting void or hole size on the shock initiation of heterogeneous explosive charges of TNT. Shocks interacting with TNT containing various hole sizes have been modeled. The void fraction was held at 0.5% while the spherical hole sizes were varied from 0.5- to 0.0005-mm-radius and the TNT was shocked to 12.5 GPa. As the hole size was varied from 0.5 to 0.05 mm, the explosive became more sensitive to shock as the hole size decreased, and the number of hot spots increased. Decreasing the hole size to 0.0005 mm resulted in failure of a 12.5-GPa shock wave to build toward propagating detonation because the resulting hot spots were cooled by side rarefactions before appreciable decomposition occurred.

As observed experimentally, the hydrodynamic hot-spot model indicates that at the same density, the most shock-sensitive explosive will be that with particle sizes between the coarse and extremely fine particle sizes. The hydrodynamic hot-spot model describes basic features of the particle-size effect on the shock initiation of heterogeneous explosives. Increased hole size results in larger hot spots that decompose more of the explosive and result in increased sensitivity of the explosive to shock. Increased numbers of holes result in more hot spots that decompose more explosive and increase the sensitivity of the explosive to shock. The interaction between hole size and number of holes is complicated and requires numerical modeling for evaluation of specific cases. The hole size can become sufficiently small that the hot spot is cooled by side rarefactions before appreciable decomposition can occur. Because increasing the number of holes while holding constant the percentage of voids results in smaller holes, we have competing processes that may result in either a more or less shock-sensitive explosive. The magnitude of the competing processes will change as the initial shock pressure is changed, resulting in reversals of the relative shock sensitivity of explosives with different particle sizes such as observed with low-pressure gap sensitivity and high-pressure wedge tests (2). In low-pressure gap sensitivity tests, the coarse-particle explosive is often

more sensitive than the fine-particle explosive. As the pressure is lowered, the fine-particle explosive forms smaller hot spots than can be more effectively cooled by side rarefactions. The coarser particle explosive forms larger hot spots than can still be effective in supporting and increasing the shock wave at low initial shock pressures. The hydrodynamic hot-spot model has resulted in an increased understanding of the effect of particle size on shock initiation properties.

REFERENCES

1. A. W. Campbell, W. C. Davis, J. B. Ramsay, and J. R. Travis, "Shock Initiation of Solid Explosives," *Physics of Fluids* 4, 511-521 (1961).
2. Donna Price, "Effect of Particle Size on the Sensitivity of Pure Porous HE," *Journal of Energetic Materials* 6 (1988).
3. H. Moulard, J. W. Kury, and A. Delclos, "The Effect of RDX Particle Size on the Shock Sensitivity of Cast PBX Formulations," Eighth Symposium (International) on Detonation, NSWC-MP 86-194, 902-913 (1985).
4. Charles L. Mader, *Numerical Modeling of Detonation* (University of California Press, Berkeley, 1979).
5. Charles L. Mader and James D. Kershner, "Three-Dimensional Modeling of Shock Initiation of Heterogeneous Explosives," Nineteenth Symposium (International) on Combustion, Williams and Wilkins, Eds., 685-690 (1982).
6. Charles L. Mader and James D. Kershner, "The Three-Dimensional Hydrodynamic Hot Spot Model," Eighth Symposium (International) on Detonation, NSWC-MP 86-194, 42-51 (1985).
7. Charles L. Mader and James D. Kershner, "Three-Dimensional Eulerian Calculations of Triple-Wave-Initiated PBX-9404," Los Alamos National Laboratory report LA-8206 (1980).
8. Charles L. Mader, "Detonation Wave Interactions," Seventh Symposium (International) on Detonation, NSWC-MP 82-334, 669-677 (1981).
9. Charles L. Mader, James D. Kershner, and George H. Pimbley, "Three-Dimensional Modeling of Inert Metal Loaded Explosives," *Journal of Energetic Materials* 1, 293-324 (1983).
10. Charles L. Mader and James D. Kershner, "Numerical Modeling of the Reaction Zone in Heterogeneous Explosives," *Journal of Energetic Materials* 5, 143-155 (1987).
11. Charles L. Mader, "Detonation Properties of Condensed Explosives Computed using the Becker-Kistiakowsky-Wilson Equation of State," Los Alamos Scientific Laboratory report LA-2900 (1963).

Figure Captions

- Fig. 1. A single 0.5-mm-radius spherical hole in TNT. The initial shock pressure is 15.0 GPa. The density and burn fraction contours through the center of the hole are shown at various times. The resulting hot spot builds toward propagating detonation.
- Fig. 2. A single 0.5-mm-radius spherical hole in TNT. The initial shock pressure is 12.5 GPa. The density and burn fraction contours through the center of the hole are shown at various times. The resulting hot spot is marginally failing.
- Fig. 3. A single 0.05-mm-radius spherical hole in TNT. The initial shock pressure is 15.0 GPa. The density and burn fraction contours through the center of the hole are shown at various times. The resulting hot spot is failing to build to detonation.
- Fig. 4. A matrix of 0.5% air holes in TNT. The spherical air holes have diameters of 0.5 mm. The initial shock pressure is 12.5 GPa. The density and burn fraction contours through the center of the matrix are shown at various times. The flow builds toward a propagating detonation.
- Fig. 5. A matrix of 0.5% air holes in TNT. The spherical air holes have diameters of 0.05 mm. The initial shock pressure is 12.5 GPa. The density and burn fraction contours through the center of the matrix are shown at various times. The flow quickly builds toward a propagating detonation.
- Fig. 6. A matrix of 0.5% air holes in TNT. The spherical air holes have diameters of 0.0005 mm. The initial shock pressure is 12.5 GPa. The density and burn fraction contours through the center of the matrix are shown at various times. The flow fails to result in appreciable decomposition of the explosive.

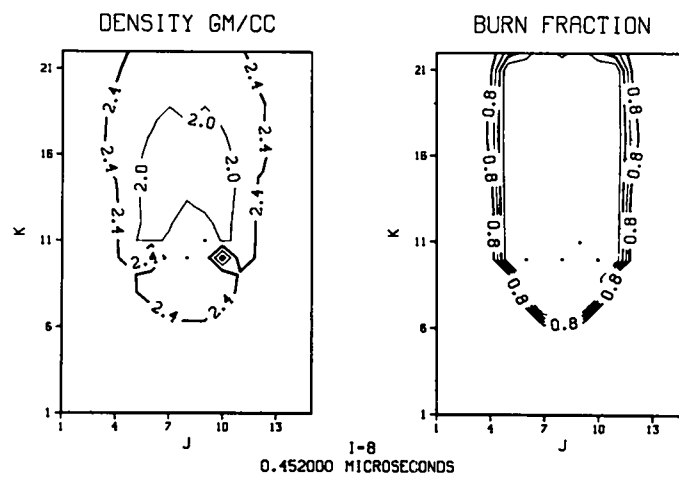
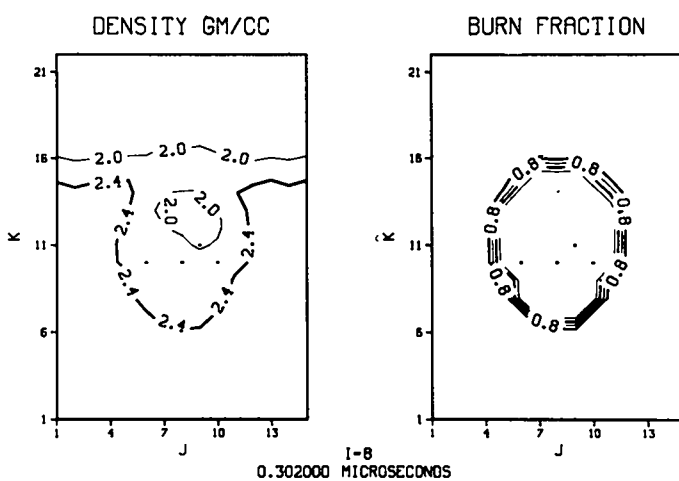
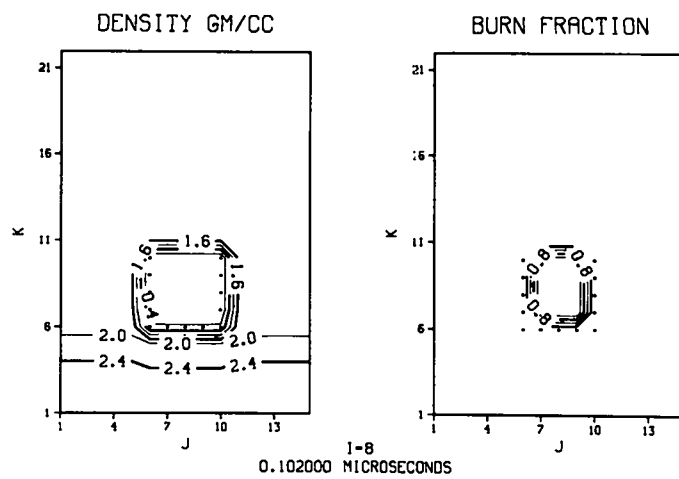


Fig. 1. A single 0.5-mm-radius spherical hole in TNT. The initial shock pressure is 15.0 GPa. The density and burn fraction contours through the center of the hole are shown at various times. The resulting hot spot builds toward propagating detonation.

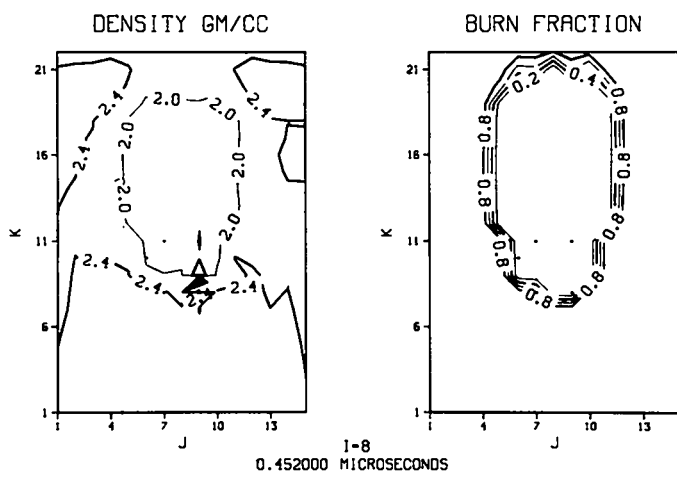
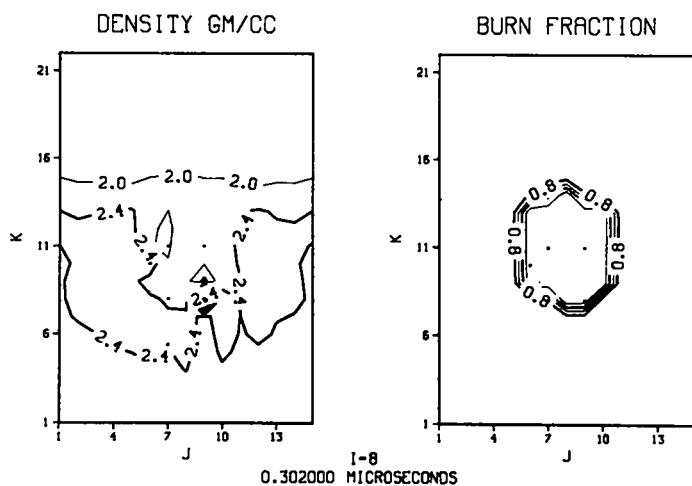
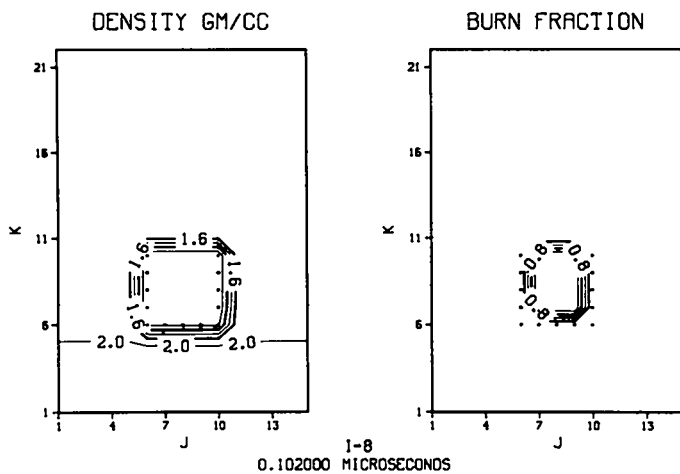


Fig. 2. A single 0.5-mm-radius spherical hole in TNT. The initial shock pressure is 12.5 GPa. The density and burn fraction contours through the center of the hole are shown at various times. The resulting hot spot is marginally failing.

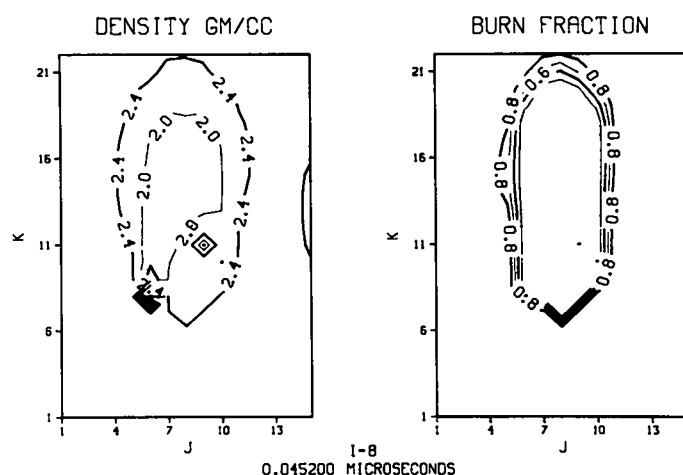
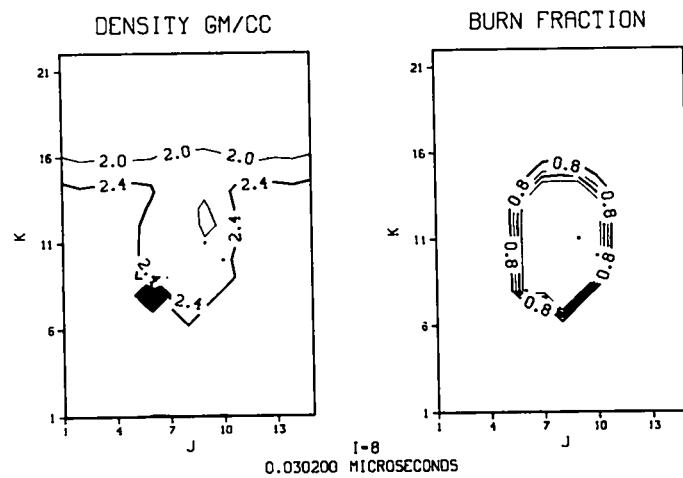
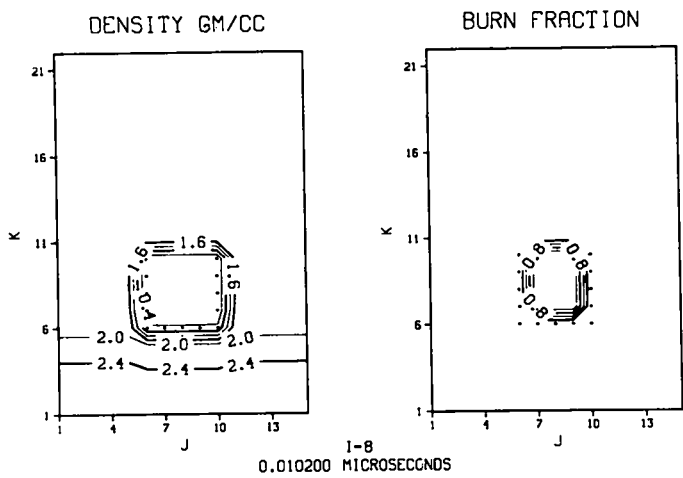


Fig. 3. A single 0.05-mm-radius spherical hole in TNT. The initial shock pressure is 15.0 GPa. The density and burn fraction contours through the center of the hole are shown at various times. The resulting hot spot is failing to build to detonation.

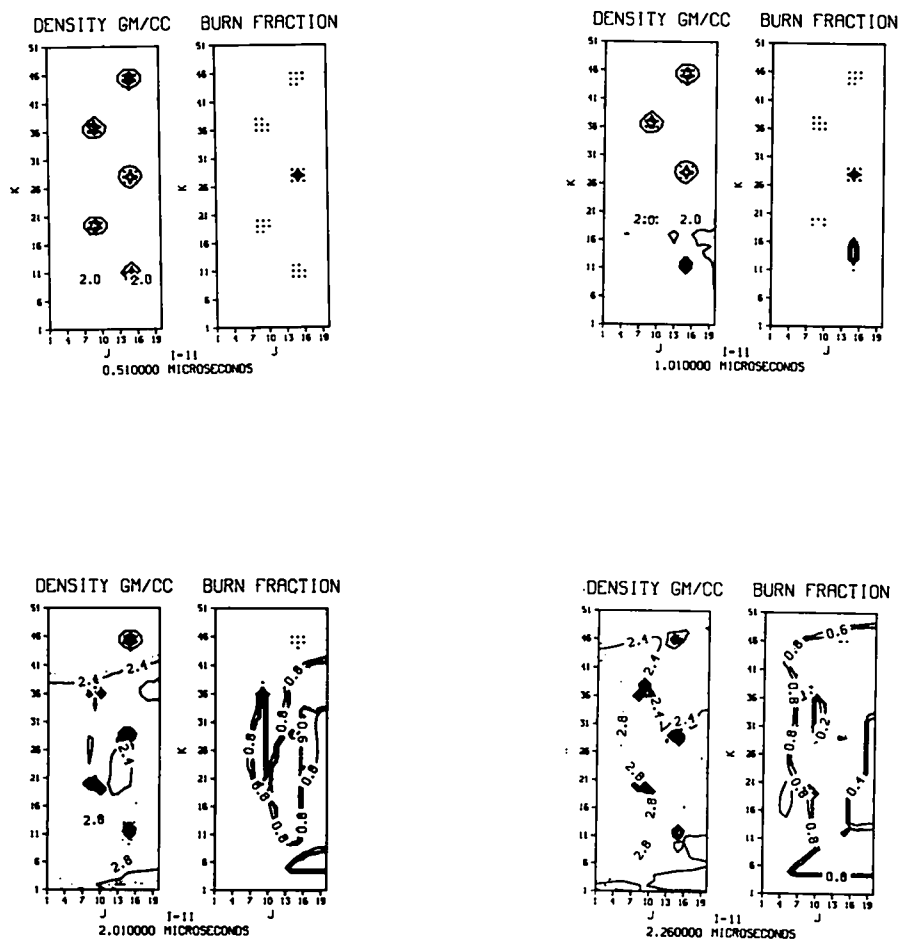


Fig. 4. A matrix of 0.5% air holes in TNT. The spherical air holes have diameters of 0.5-mm. The initial shock pressure is 12.5 GPa. The density and burn fraction contours through the center of the matrix are shown at various times. The flow builds toward a propagating detonation.

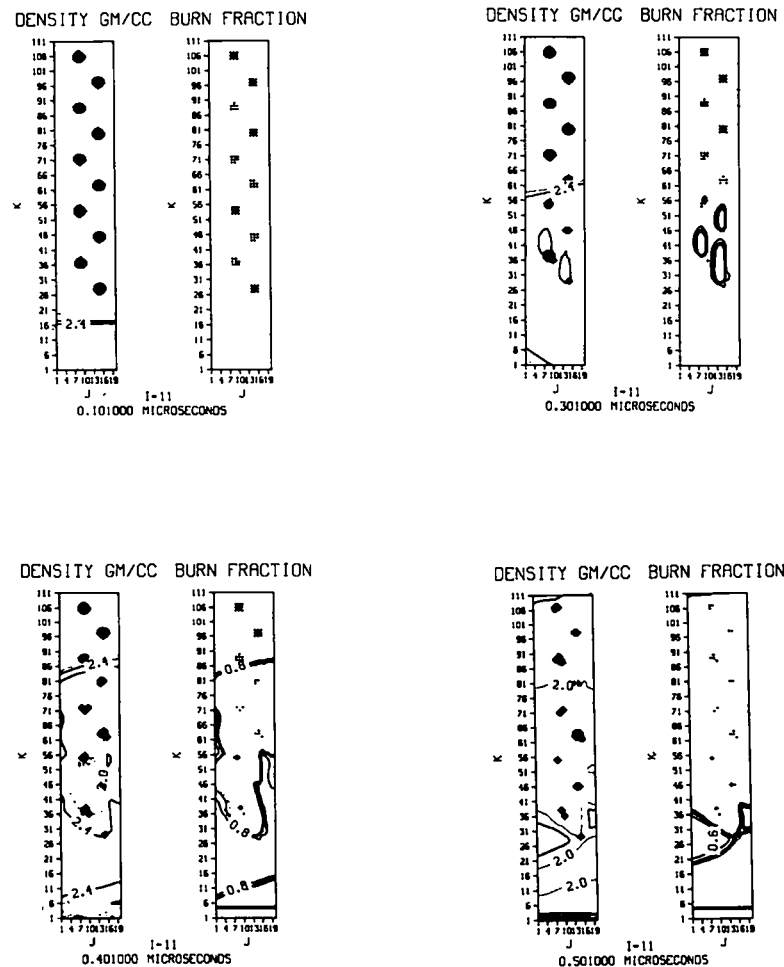


Fig. 5. A matrix of 0.5% air holes in TNT. The spherical air holes have diameters of 0.05-mm. The initial shock pressure is 12.5 GPa. The density and burn fraction contours through the center of the matrix are shown at various times. The flow quickly builds toward a propagating detonation.

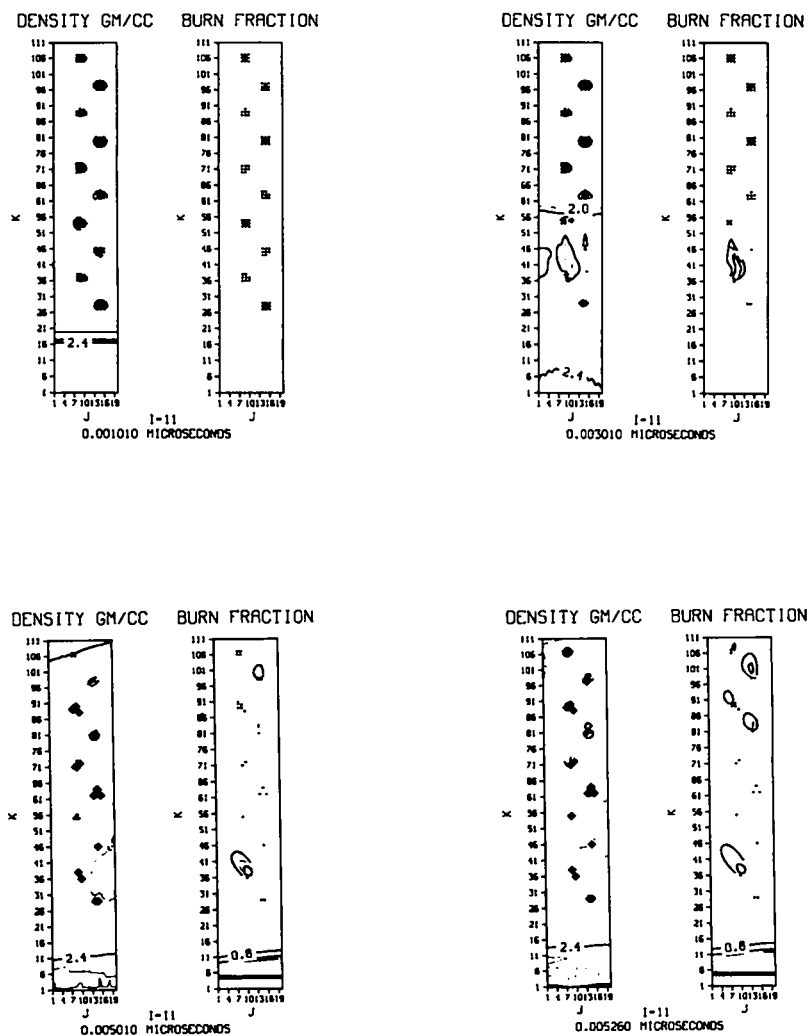


Fig. 6. A matrix of 0.5% air holes in TNT. The spherical air holes have diameters of 0.0005-mm. The initial shock pressure is 12.5 GPa. The density and burn fraction contours through the center of the matrix are shown at various times. The flow fails to result in appreciable decomposition of the explosive.

Table 2. The TNT Nonreactive Hugoniot

SOLID EQUATION OF STATE CALCULATION FOR NON REACTIVE TNT FOR HOT SPOT STUDY

US = 2.2000000000E-01 + 1.76600000000E+00 S FROM P0 TO 1.05000000000E+00 MEGABARS

THE INITIAL DENSITY IS 1.6400000000E+00 GM/CC

THE COMPRESSIBILITY IS 1.1530000000E+01

THE LINEAR COEFFICIENT OF EXPANSION IS 5.0000000000E-05

THE INITIAL TEMPERATURE IS 3.0000000000E+02

THE HEAT CAPACITY IS 2.9300000000E-01

THE VOLUME INCREMENT IS 1.0000000000E-04

THE TEMPERATURE FIT IS BETWEEN 1.0000000000E-04 AND 1.0000000000E+00 MEGABARS

LN(T) = -2.71235359951E+00 -4.86625796696E+01 LNV -1.02215618376E+02 LNV*2 -9.01182904938E+01 LNV*3 -2.60329744463E+01 LNV*4

VOLUME IN CC/GM	PRESSURE IN MEGABARS	TEMPERATURE DEG K	SHOCK VELOCITY	PARTICLE VELOCITY
6.09756097561E-01	0.	3.0000000000E+02	2.2000000000E-01	0.
6.08756097561E-01	1.30933974130E-04	3.00318402278E+02	2.20639023566E-01	3.61847998659E-04
6.07756097561E-01	2.63395872986E-04	3.00637204931E+02	2.21281770228E-01	7.25804206373E-04
6.06756097561E-01	3.97405814005E-04	3.00956472352E+02	2.21928272621E-01	1.09188710133E-03
6.05756097561E-01	5.32984229470E-04	3.01276270680E+02	2.22578563758E-01	1.46011537830E-03
6.04756097561E-01	6.70151872308E-04	3.01596667844E+02	2.23232677043E-01	1.83050795181E-03
6.03756097561E-01	8.08929821995E-04	3.01917733604E+02	2.23890646272E-01	2.20308395939E-03
6.02756097561E-01	9.49339490608E-04	3.02239539595E+02	2.24552505643E-01	2.57786276486E-03
6.01756097561E-01	1.09140262898E-03	3.02562159374E+02	2.25218289756E-01	2.95486396170E-03
6.00756097561E-01	1.23514133303E-03	3.02885568461E+02	2.25888033627E-01	3.33410737644E-03
5.99756097561E-01	1.38057805016E-03	3.03210144388E+02	2.26561772685E-01	3.71561307216E-03
5.98756097561E-01	1.52773558586E-03	3.03535666747E+02	2.27239542788E-01	4.09940135203E-03
5.97756097561E-01	1.67663711042E-03	3.03862317237E+02	2.27921380219E-01	4.48549276286E-03
5.96756097561E-01	1.82730616580E-03	3.04190179720E+02	2.28607321703E-01	4.87390809886E-03
5.95756097561E-01	1.97976667262E-03	3.04519340263E+02	2.29297404404E-01	5.26466840528E-03
5.94756097560E-01	2.13404293736E-03	3.04849887201E+02	2.29991665939E-01	5.65779498228E-03
5.93756097560E-01	2.29015965967E-03	3.05181911184E+02	2.30690144381E-01	6.05330938875E-03
5.92756097560E-01	2.44814193982E-03	3.05515505233E+02	2.31392878266E-01	6.45123344627E-03
5.91756097560E-01	2.60801528641E-03	3.05850764803E+02	2.32099906603E-01	6.85158924316E-03
5.90756097560E-01	2.76980562415E-03	3.06187787832E+02	2.32811268879E-01	7.25439913850E-03
5.89756097560E-01	2.93353930185E-03	3.06526674809E+02	2.33527005063E-01	7.65968576633E-03
5.88756097560E-01	3.09924310060E-03	3.06867528830E+02	2.34247155622E-01	8.06747203991E-03
5.87756097560E-01	3.26694424210E-03	3.07210455664E+02	2.34971761521E-01	8.47778115598E-03
5.86756097560E-01	3.43667039724E-03	3.07555563815E+02	2.35700864234E-01	8.89063659921E-03
5.85756097560E-01	3.60844969478E-03	3.07902964590E+02	2.36434505751E-01	9.30606214667E-03
5.84756097560E-01	3.78231073030E-03	3.08252772166E+02	2.37172728587E-01	9.72408187237E-03
5.83756097560E-01	3.95828257531E-03	3.08605103657E+02	2.37915575788E-01	1.01447201520E-02
5.82756097560E-01	4.13639478659E-03	3.08960079192E+02	2.38663090945E-01	1.05680016674E-02
5.81756097560E-01	4.31667741575E-03	3.09317821979E+02	2.39415318193E-01	1.09939514118E-02
5.80756097560E-01	4.49916101895E-03	3.09678458388E+02	2.40172302230E-01	1.14225946945E-02
5.79756097560E-01	4.68387666692E-03	3.10042118023E+02	2.40934088319E-01	1.18539571457E-02
5.78756097560E-01	4.87085595515E-03	3.10408933804E+02	2.41700722299E-01	1.22880647221E-02
5.77756097560E-01	5.06013101434E-03	3.10779042044E+02	2.42472250595E-01	1.27249437116E-02
5.76756097560E-01	5.25173452111E-03	3.11152582537E+02	2.43248720225E-01	1.31646207390E-02
5.75756097560E-01	5.44569970888E-03	3.11529698638E+02	2.44030178814E-01	1.36071227111E-02
5.74756097560E-01	5.64206037912E-03	3.11910537357E+02	2.44816674598E-01	1.40524771224E-02
5.73756097560E-01	5.84085091274E-03	3.12295249440E+02	2.45608256440E-01	1.45007114607E-02
5.72756097560E-01	6.04210628186E-03	3.12683989470E+02	2.46404973833E-01	1.49518538127E-02
5.71756097560E-01	6.24586206174E-03	3.13076915956E+02	2.47206876919E-01	1.54059325701E-02
5.70756097560E-01	6.45215444310E-03	3.13474191431E+02	2.48014016491E-01	1.58629764953E-02
5.69756097560E-01	6.66102024465E-03	3.13875982552E+02	2.48826444009E-01	1.63230147275E-02
5.68756097560E-01	6.87249692594E-03	3.14282460203E+02	2.49644211610E-01	1.67860767892E-02

5.67756097560E-01	7.08662260054E-03	3.14693799598E+02	2.50467372118E-01	1.72521925920E-02
5.66756097560E-01	7.30343604950E-03	3.15110180390E+02	2.51295979055E-01	1.77213924436E-02
5.65756097560E-01	7.52297673517E-03	3.15531786784E+02	2.52130086657E-01	1.81937070538E-02
5.64756097559E-01	7.74528481527E-03	3.1598807643E+02	2.52969749879E-01	1.86691675417E-02
5.63756097559E-01	7.97040115739E-03	3.16391436615E+02	2.53815024411E-01	1.91478054422E-02
5.62756097559E-01	8.19836735382E-03	3.16829872243E+02	2.54665966692E-01	1.96296527132E-02
5.61756097559E-01	8.42922573667E-03	3.17274318094E+02	2.55522633918E-01	2.01147417427E-02
5.60756097559E-01	8.66301939345E-03	3.17724982883E+02	2.56385084058E-01	2.06031053556E-02
5.59756097559E-01	8.89979218295E-03	3.18182080605E+02	2.57253375867E-01	2.10947768218E-02
5.58756097559E-01	9.13958875158E-03	3.18645830664E+02	2.58127568899E-01	2.15897898634E-02
5.57756097559E-01	9.38245455004E-03	3.19116458013E+02	2.59007723518E-01	2.20881786623E-02
5.56756097559E-01	9.62843585046E-03	3.19594193295E+02	2.59893900915E-01	2.25899778683E-02
5.55756097559E-01	9.87757976390E-03	3.20079272986E+02	2.60786163124E-01	2.30952226070E-02
5.54756097559E-01	1.01299342584E-02	3.20517939544E+02	2.61684573030E-01	2.36039484881E-02
5.53756097559E-01	1.03855481772E-02	3.21072441559E+02	2.62589194389E-01	2.41161916135E-02
5.52756097559E-01	1.06444712579E-02	3.21581033916E+02	2.63500091843E-01	2.46319885863E-02
5.51756097559E-01	1.09067541515E-02	3.22097977950E+02	2.64417330933E-01	2.51513765192E-02
5.50756097559E-01	1.11724484426E-02	3.22623541613E+02	2.65340978114E-01	2.56743930432E-02
5.49756097559E-01	1.14416066693E-02	3.231517999647E+02	2.66271100776E-01	2.62010763173E-02
5.48756097559E-01	1.17142823444E-02	3.23701633755E+02	2.67207767256E-01	2.67314650371E-02
5.47756097559E-01	1.19905299764E-02	3.24254732783E+02	2.68151046854E-01	2.72655984450E-02
5.46756097559E-01	1.22704050920E-02	3.24817592907E+02	2.69101009855E-01	2.78035163391E-02
5.45756097559E-01	1.25539642578E-02	3.25390517816E+02	2.70057727542E-01	2.83452590837E-02
5.44756097559E-01	1.28412651040E-02	3.25973818915E+02	2.71021272215E-01	2.88908676191E-02
5.43756097559E-01	1.31323663477E-02	3.26567815523E+02	2.71991717211E-01	2.94403834719E-02
5.42756097559E-01	1.34273278173E-02	3.27172835080E+02	2.72969136920E-01	2.99938487658E-02
5.41756097559E-01	1.37262104772E-02	3.27789213357E+02	2.73953606806E-01	3.05513062320E-02
5.40756097559E-01	1.40290764536E-02	3.28417294678E+02	2.74945203423E-01	3.11127992204E-02
5.39756097559E-01	1.43359890603E-02	3.29057432147E+02	2.75944004442E-01	3.16783717109E-02
5.38756097559E-01	1.46470128260E-02	3.29709987870E+02	2.76950088662E-01	3.22480683248E-02
5.37756097559E-01	1.49622135216E-02	3.30375333206E+02	2.77963536038E-01	3.28219343365E-02
5.36756097559E-01	1.52816581883E-02	3.31053849000E+02	2.78984427700E-01	3.34000156854E-02
5.35756097559E-01	1.560514151674E-02	3.31745925843E+02	2.80012845974E-01	3.39823589885E-02
5.34756097559E-01	1.59335541291E-02	3.32451964329E+02	2.81048874402E-01	3.45690115526E-02
5.33756097559E-01	1.62661461040E-02	3.33172375320E+02	2.82092597770E-01	3.51600213872E-02
5.32756097559E-01	1.66032635141E-02	3.33907580222E+02	2.83144102126E-01	3.57554372177E-02
5.31756097559E-01	1.69449802051E-02	3.34658011272E+02	2.84203474809E-01	3.63553084987E-02
5.30756097559E-01	1.72913714794E-02	3.354241111820E+02	2.85270804465E-01	3.69596854278E-02
5.29756097559E-01	1.76425141307E-02	3.36206336639E+02	2.86346181082E-01	3.75686189592E-02
5.28756097559E-01	1.79984864782E-02	3.37005152226E+02	2.87429696006E-01	3.81821608187E-02
5.27756097559E-01	1.83593684031E-02	3.37821037123E+02	2.88521441972E-01	3.88003635177E-02
5.26756097559E-01	1.87252413853E-02	3.38654482245E+02	2.89621513131E-01	3.94232803687E-02
5.25756097559E-01	1.90961885411E-02	3.39505991214E+02	2.90730005073E-01	4.00509655002E-02
5.24756097559E-01	1.94722946623E-02	3.40376080710E+02	2.91847014859E-01	4.06834738727E-02
5.23756097559E-01	1.98536462566E-02	3.41265280826E+02	2.92972641046E-01	4.13208612945E-02
5.22756097559E-01	2.02403315878E-02	3.42174135437E+02	2.94106983718E-01	4.19631844383E-02
5.21756097559E-01	2.06324407192E-02	3.43103202581E+02	2.95250144515E-01	4.26105008578E-02
5.20756097559E-01	2.10300655562E-02	3.44053054848E+02	2.96402226663E-01	4.32628690052E-02
5.19756097559E-01	2.14332998911E-02	3.45024279783E+02	2.97563335007E-01	4.39203482485E-02
5.18756097559E-01	2.18422394496E-02	3.46017480306E+02	2.98733576039E-01	4.45829988895E-02
5.17756097559E-01	2.22569819374E-02	3.47033275133E+02	2.99913057935E-01	4.52508821827E-02
5.16756097559E-01	2.26776270890E-02	3.48072299222E+02	3.01101890584E-01	4.59240603534E-02
5.15756097559E-01	2.31042767176E-02	3.49135204229E+02	3.02300185627E-01	4.66025966178E-02
5.14756097559E-01	2.35370347666E-02	3.50222658973E+02	3.03508056487E-01	4.72865552023E-02
5.13756097559E-01	2.39760073624E-02	3.51335349922E+02	3.04725618409E-01	4.79760013638E-02
5.12756097559E-01	2.44213028686E-02	3.52473981692E+02	3.05952988492E-01	4.86710014109E-02
5.11756097559E-01	2.48730319424E-02	3.53639277562E+02	3.07190285731E-01	4.93716227244E-02
5.10756097559E-01	2.53313075916E-02	3.54831980001E+02	3.08437631055E-01	5.00779337798E-02
5.09756097559E-01	2.57962452342E-02	3.56052851221E+02	3.09695147363E-01	5.07900041692E-02
5.08756097559E-01	2.62679627594E-02	3.57302673737E+02	3.10962959567E-01	5.15079046243E-02
5.07756097559E-01	2.67465805902E-02	3.58582250951E+02	3.12241194632E-01	5.22317070398E-02
5.06756097559E-01	2.72322217483E-02	3.59892407754E+02	3.13529981622E-01	5.29614844974E-02
5.05756097559E-01	2.77250119203E-02	3.61233991145E+02	3.14829451739E-01	5.36973112903E-02
5.04756097557E-01	2.82250795266E-02	3.62607870873E+02	3.16139738367E-01	5.44392629487E-02

5.03756097557E-01	2.87325557917E-02	3.64014940098E+02	3.17460977124E-01	5.51874162651E-02
5.02756097557E-01	2.92475748169E-02	3.65456116068E+02	3.18793305902E-01	5.59418493215E-02
5.01756097557E-01	2.97702736555E-02	3.66932340834E+02	3.20136864917E-01	5.67026415160E-02
5.00756097557E-01	3.03007923896E-02	3.68444581966E+02	3.21491796762E-01	5.74698735910E-02
4.99756097557E-01	3.08392742097E-02	3.69993833312E+02	3.22858246450E-01	5.82436276616E-02
4.98756097557E-01	3.13858654968E-02	3.71581115771E+02	3.24236361474E-01	5.90239872447E-02
4.97756097557E-01	3.19407159066E-02	3.73207478095E+02	3.25626291853E-01	5.98110372896E-02
4.96756097557E-01	3.25039784566E-02	3.74873997714E+02	3.27028190192E-01	6.06048642084E-02
4.95756097557E-01	3.30758096157E-02	3.76581781598E+02	3.28442211733E-01	6.14055559075E-02
4.94756097557E-01	3.36563693971E-02	3.78331967132E+02	3.29868514415E-01	6.22132018208E-02
4.93756097557E-01	3.42458214532E-02	3.80125723040E+02	3.31307258935E-01	6.30278929419E-02
4.92756097557E-01	3.48443331741E-02	3.81964250317E+02	3.32758608803E-01	6.38497218593E-02
4.91756097557E-01	3.54520757894E-02	3.83848783215E+02	3.34222730408E-01	6.46787827907E-02
4.90756097557E-01	3.60692244724E-02	3.85780590246E+02	3.35699793080E-01	6.55151716196E-02
4.89756097557E-01	3.66959584482E-02	3.87760975228E+02	3.37189969156E-01	6.63589859320E-02
4.88756097557E-01	3.73324611053E-02	3.89791278363E+02	3.38693434046E-01	6.72103250541E-02
4.87756097557E-01	3.79789201104E-02	3.91872877351E+02	3.40210366302E-01	6.80692900919E-02
4.86756097557E-01	3.86355275272E-02	3.94007188546E+02	3.41740947692E-01	6.89359839706E-02
4.85756097557E-01	3.93024799388E-02	3.96195668147E+02	3.43285363267E-01	6.98105114761E-02
4.84756097557E-01	3.99799785740E-02	3.98439813438E+02	3.44843801439E-01	7.06929792971E-02
4.83756097557E-01	4.066822944384E-02	4.00741164060E+02	3.46416454057E-01	7.15834960686E-02
4.82756097557E-01	4.13674434488E-02	4.03101303337E+02	3.48003516487E-01	7.24821724161E-02
4.81756097557E-01	4.20778365726E-02	4.05521859645E+02	3.49605187690E-01	7.33891210021E-02
4.80756097557E-01	4.27996299717E-02	4.08004507829E+02	3.51221670307E-01	7.43044565724E-02
4.79756097557E-01	4.35330501513E-02	4.10550970667E+02	3.52853170745E-01	7.52282960051E-02
4.78756097557E-01	4.42783291132E-02	4.13163020395E+02	3.54499899264E-01	7.61607583602E-02
4.77756097557E-01	4.50357045149E-02	4.15842480275E+02	3.56162070067E-01	7.71019649305E-02
4.76756097557E-01	4.58054198333E-02	4.18591226227E+02	3.57839901394E-01	7.80520392944E-02
4.75756097557E-01	4.65877245347E-02	4.21411188518E+02	3.59533615615E-01	7.90111073700E-02
4.74756097557E-01	4.73828742499E-02	4.24304353510E+02	3.61243439333E-01	7.99792974708E-02
4.73756097557E-01	4.819111309556E-02	4.27272765473E+02	3.62969603481E-01	8.09567403627E-02
4.72756097557E-01	4.90127631621E-02	4.30318528463E+02	3.64712343425E-01	8.19435693230E-02
4.71756097557E-01	4.98480461070E-02	4.33443808270E+02	3.66471899075E-01	8.29399202012E-02
4.70756097557E-01	5.06972619565E-02	4.36650834435E+02	3.68248514995E-01	8.39459314807E-02
4.69756097557E-01	5.15607000125E-02	4.39941902347E+02	3.70042440511E-01	8.49617443439E-02
4.68756097557E-01	5.24386569276E-02	4.43319375406E+02	3.71853929834E-01	8.59875027374E-02
4.67756097557E-01	5.33314369282E-02	4.46785687285E+02	3.73683242176E-01	8.70233534404E-02
4.66756097557E-01	5.42393520439E-02	4.50343344255E+02	3.75530641874E-01	8.80694461349E-02
4.65756097557E-01	5.51627223470E-02	4.53994927615E+02	3.77396398521E-01	8.91259334773E-02
4.64756097557E-01	5.61018761984E-02	4.57743096203E+02	3.79280787091E-01	9.01929711729E-02
4.63756097557E-01	5.70571505043E-02	4.61590589008E+02	3.81184088081E-01	9.12707180528E-02
4.62756097557E-01	5.80288909808E-02	4.65540227877E+02	3.83106587644E-01	9.23593361519E-02
4.61756097557E-01	5.90174524285E-02	4.69594920327E+02	3.85048577737E-01	9.34589907910E-02
4.60756097557E-01	6.00231990169E-02	4.73757662468E+02	3.87010356265E-01	9.45698506596E-02
4.59756097557E-01	6.10465045797E-02	4.78031542035E+02	3.88992272373E-01	9.56920879029E-02
4.58756097557E-01	6.20877529203E-02	4.82419741536E+02	3.90994500920E-01	9.68258782105E-02
4.57756097557E-01	6.31473381289E-02	4.86925541528E+02	3.93017494003E-01	9.79714009079E-02
4.56756097557E-01	6.42256649111E-02	4.91552324019E+02	3.95061529765E-01	9.91288390513E-02
4.55756097557E-01	6.53231489290E-02	4.96303575999E+02	3.97126938241E-01	1.00298379525E-01
4.54756097557E-01	6.64402171551E-02	5.01182893119E+02	3.99214056409E-01	1.01480213142E-01
4.53756097557E-01	6.75773082393E-02	5.06193983508E+02	4.01323228364E-01	1.02674534748E-01
4.52756097557E-01	6.87348728898E-02	5.11340671747E+02	4.03454805516E-01	1.03881543327E-01
4.51756097557E-01	6.99133742687E-02	5.16626903001E+02	4.05609146776E-01	1.05101442116E-01
4.50756097557E-01	7.11132884023E-02	5.22056747316E+02	4.07786618766E-01	1.06334438712E-01
4.49756097557E-01	7.23351046078E-02	5.27634404091E+02	4.09987596021E-01	1.07580745199E-01
4.48756097557E-01	7.35793259360E-02	5.33364206735E+02	4.12212461208E-01	1.08840578260E-01
4.47756097557E-01	7.48464696313E-02	5.39250627505E+02	4.14461605342E-01	1.10114159310E-01
4.46756097557E-01	7.61370676097E-02	5.45298282556E+02	4.16735428022E-01	1.11401714622E-01
4.45756097556E-01	7.74516669557E-02	5.51511937185E+02	4.19034337665E-01	1.12703475461E-01
4.44756097556E-01	7.87908304385E-02	5.57896511307E+02	4.21358751747E-01	1.14019678226E-01
4.43756097556E-01	8.01551370491E-02	5.64457085146E+02	4.2370907060E-01	1.15350564587E-01
4.42756097556E-01	8.15451825584E-02	5.71198905174E+02	4.26085809974E-01	1.16696381639E-01
4.41756097556E-01	8.29615800983E-02	5.78127390297E+02	4.28489336703E-01	1.18057382052E-01
4.40756097556E-01	8.44049607656E-02	5.85248138301E+02	4.30920133587E-01	1.19433824228E-01

4.39756097556E-01	8.58759742507E-02	5.92566932576E+02	4.33378667380E-01	1.20825972469E-01
4.38756097556E-01	8.73752894923E-02	6.00089749127E+02	4.35865415549E-01	1.22234097140E-01
4.37756097556E-01	8.89035953584E-02	6.07822763882E+02	4.38380866584E-01	1.23658474849E-01
4.36756097556E-01	9.04616013557E-02	6.15772360325E+02	4.40925520316E-01	1.25099388627E-01
4.35756097556E-01	9.20500383686E-02	6.23945137453E+02	4.43499888250E-01	1.26557128114E-01
4.34756097556E-01	9.36696594291E-02	6.32347918083E+02	4.46104493907E-01	1.28031989755E-01
4.33756097556E-01	9.53212405184E-02	6.40987757529E+02	4.48739873177E-01	1.29524276997E-01
4.32756097556E-01	9.70055814033E-02	6.49871952657E+02	4.51406574692E-01	1.31034300505E-01
4.31756097556E-01	9.87235065077E-02	6.59008051341E+02	4.54105160200E-01	1.32562378369E-01
4.30756097556E-01	1.00475865821E-01	6.68403862352E+02	4.56836204963E-01	1.34108836333E-01
4.29756097556E-01	1.02263535847E-01	6.78067465680E+02	4.59600298168E-01	1.35674008023E-01
4.28756097556E-01	1.04087420592E-01	6.88007223329E+02	4.62398043347E-01	1.37258235191E-01
4.27756097556E-01	1.05948452596E-01	6.98231790600E+02	4.65230058815E-01	1.38861867959E-01
4.26756097556E-01	1.07847594013E-01	7.08750127894E+02	4.68096978133E-01	1.40485265081E-01
4.25756097556E-01	1.09785837731E-01	7.19571513053E+02	4.70999450572E-01	1.42128794208E-01
4.24756097556E-01	1.11764208553E-01	7.30705554276E+02	4.73938141608E-01	1.43792832168E-01
4.23756097556E-01	1.13783764416E-01	7.42162203633E+02	4.76913733430E-01	1.45477765249E-01
4.22756097556E-01	1.15845597682E-01	7.53951771213E+02	4.79926925468E-01	1.47183989506E-01
4.21756097556E-01	1.17950836470E-01	7.66084939940E+02	4.82978434940E-01	1.48911911065E-01
4.20756097556E-01	1.20100646063E-01	7.78572781085E+02	4.86068997421E-01	1.50661946444E-01
4.19756097556E-01	1.22296230370E-01	7.91426770528E+02	4.89199367436E-01	1.52434522897E-01
4.18756097556E-01	1.24538833460E-01	8.04658805785E+02	4.92370319073E-01	1.54230078750E-01
4.17756097556E-01	1.26829741164E-01	8.18281223872E+02	4.95582646622E-01	1.56049063772E-01
4.16756097556E-01	1.29170282759E-01	8.32306820022E+02	4.98837165235E-01	1.57891939544E-01
4.15756097556E-01	1.31561823217E-01	8.46748867329E+02	5.02134711621E-01	1.59759179853E-01
4.14756097556E-01	1.34005812549E-01	8.61621137347E+02	5.05476144759E-01	1.61651271098E-01
4.13756097556E-01	1.36503692739E-01	8.76937921712E+02	5.08862346646E-01	1.63568712710E-01
4.12756097556E-01	1.39056994758E-01	8.92714054842E+02	5.12294223071E-01	1.65512017594E-01
4.11756097556E-01	1.41667293181E-01	9.08964937772E+02	5.15772704426E-01	1.67481712585E-01
4.10756097556E-01	1.44336217912E-01	9.25706563189E+02	5.19298746544E-01	1.69478338926E-01
4.09756097556E-01	1.47065456512E-01	9.42955541742E+02	5.22873331577E-01	1.71502452762E-01
4.08756097556E-01	1.49856756643E-01	9.60729129688E+02	5.26497468906E-01	1.73554625654E-01
4.07756097556E-01	1.52711928633E-01	9.79045257968E+02	5.30172196092E-01	1.75635445126E-01
4.06756097556E-01	1.55632848167E-01	9.97922562784E+02	5.33898579868E-01	1.77745515214E-01
4.05756097556E-01	1.58621459123E-01	1.01738041776E+03	5.37677717169E-01	1.79885457061E-01
4.04756097556E-01	1.61679776534E-01	1.03743896782E+03	5.41510736209E-01	1.82055909518E-01
4.03756097556E-01	1.64809889721E-01	1.05811916481E+03	5.45398797604E-01	1.84257529787E-01
4.02756097556E-01	1.68013965567E-01	1.07944280504E+03	5.49343095547E-01	1.86490994081E-01
4.01756097556E-01	1.71294251981E-01	1.10143256884E+03	5.53344859025E-01	1.88756998315E-01
4.00756097556E-01	1.74653081523E-01	1.12411206227E+03	5.57405353099E-01	1.91056258833E-01
3.99756097556E-01	1.78092875233E-01	1.14750586099E+03	5.61525880239E-01	1.93389513159E-01
3.98756097556E-01	1.816161446656E-01	1.17163955669E+03	5.65707781713E-01	1.95757520789E-01
3.97756097556E-01	1.85225506083E-01	1.19653980593E+03	5.69952439046E-01	1.98161064012E-01
3.96756097556E-01	1.88923665018E-01	1.22223438180E+03	5.74261275538E-01	2.00600948776E-01
3.95756097556E-01	1.92713440892E-01	1.24875222835E+03	5.78635757861E-01	2.03078005584E-01
3.94756097556E-01	1.96597762027E-01	1.27612351821E+03	5.83077397717E-01	2.05593090440E-01
3.93756097556E-01	2.00579672872E-01	1.30437971340E+03	5.87587753584E-01	2.08147085835E-01
3.92756097556E-01	2.04662339542E-01	1.33355362959E+03	5.92168432537E-01	2.10740901777E-01
3.91756097556E-01	2.08849055643E-01	1.36367950414E+03	5.96821092160E-01	2.13375476874E-01
3.90756097556E-01	2.13143248449E-01	1.39479306802E+03	6.01547442541E-01	2.16051779468E-01
3.89756097556E-01	2.17548485409E-01	1.42693162194E+03	6.06349248373E-01	2.18770808818E-01
3.88756097556E-01	2.22068481037E-01	1.46013411699E+03	6.11228331149E-01	2.21533596347E-01
3.87756097556E-01	2.26707104196E-01	1.49444124003E+03	6.16186571462E-01	2.24341206943E-01
3.86756097556E-01	2.314683985801E-01	1.52989550421E+03	6.21225911428E-01	2.27194740333E-01
3.85756097556E-01	2.36356526978E-01	1.56654134493E+03	6.26348357219E-01	2.30095332513E-01
3.84756097556E-01	2.41375907701E-01	1.60442522162E+03	6.31555981725E-01	2.33044157262E-01
3.83756097556E-01	2.46531095941E-01	1.64359572578E+03	6.36850927353E-01	2.36042427720E-01
3.82756097556E-01	2.51826857370E-01	1.68410369568E+03	6.42235408967E-01	2.39091398056E-01
3.81756097556E-01	2.57268165646E-01	1.72600233816E+03	6.47711716970E-01	2.42192365215E-01
3.80756097556E-01	2.62860213327E-01	1.769347375381E+03	6.53282220563E-01	2.45346670761E-01
3.79756097556E-01	2.68608423459E-01	1.81419709621E+03	6.58949371154E-01	2.48555702805E-01
3.78756097555E-01	2.74518461879E-01	1.86061267522E+03	6.64715705959E-01	2.51820898051E-01
3.77756097555E-01	2.80596250290E-01	1.90865815600E+03	6.70583851788E-01	2.55143743935E-01
3.76756097555E-01	2.86847980168E-01	1.95840070343E+03	6.76556529038E-01	2.58525780882E-01

3.75756097555E-01	2.93280127540E-01	2.00991076326E+03	6.82636555892E-01	2.61968604695E-01
3.74756097555E-01	2.99899468732E-01	2.06326225064E+03	6.88826852760E-01	2.65473869060E-01
3.73756097555E-01	3.06713097122E-01	2.11853275124E+03	6.95130446951E-01	2.69043288194E-01
3.72756097555E-01	3.1372841000E-01	2.17580373578E+03	7.01550477614E-01	2.72678639645E-01
3.71756097555E-01	3.20953282607E-01	2.23516078926E+03	7.08090200944E-01	2.76381767239E-01
3.70756097555E-01	3.28395778438E-01	2.29669385573E+03	7.14752995698E-01	2.80154584200E-01
3.69756097555E-01	3.36064480922E-01	2.36049750006E+03	7.21542369007E-01	2.83999076448E-01
3.68756097555E-01	3.43968361570E-01	2.42667118792E+03	7.28461962537E-01	2.87917306080E-01
3.67756097555E-01	3.52116835713E-01	2.49531958545E+03	7.35515559003E-01	2.91911415064E-01
3.66756097555E-01	3.60519788955E-01	2.56655288022E+03	7.42707089059E-01	2.95983629139E-01
3.65756097555E-01	3.69187605478E-01	2.64048715253E+03	7.50040638608E-01	3.00136261952E-01
3.64756097555E-01	3.78131198349E-01	2.71724460774E+03	7.57520456539E-01	3.04371719444E-01
3.63756097555E-01	3.87362041988E-01	2.79695424513E+03	7.65150962938E-01	3.08692504495E-01
3.62756097555E-01	3.96892206986E-01	2.87975200996E+03	7.72936757798E-01	3.13101221856E-01
3.61756097555E-01	4.06734397444E-01	2.96578138671E+03	7.80882630264E-01	3.17600583388E-01
3.60756097555E-01	4.16901991084E-01	3.05519386295E+03	7.88993568459E-01	3.22193413623E-01
3.59756097555E-01	4.27409082321E-01	3.14814945779E+03	7.97274769926E-01	3.268826555677E-01
3.58756097555E-01	4.38270528591E-01	3.24481729108E+03	8.05731652734E-01	3.31671377539E-01
3.57756097555E-01	4.49502000189E-01	3.34537619672E+03	8.14369867300E-01	3.36562778765E-01
3.56756097555E-01	4.61120033943E-01	3.45001538411E+03	8.23195308976E-01	3.41560197608E-01
3.55756097555E-01	4.73142091046E-01	3.55893515214E+03	8.32214131473E-01	3.46667118614E-01
3.54756097555E-01	4.85586619438E-01	3.67234766033E+03	8.41432761163E-01	3.51887180726E-01
3.53756097555E-01	4.98473121137E-01	3.79047776254E+03	8.50857912354E-01	3.57224185931E-01
3.52756097555E-01	5.11822224974E-01	3.91356390898E+03	8.60496603599E-01	3.62682108493E-01
3.51756097555E-01	5.25655765235E-01	4.04185912298E+03	8.70356175125E-01	3.68265104828E-01
3.50756097555E-01	5.399968667686E-01	4.17563205963E+03	8.80444307476E-01	3.73977524052E-01
3.49756097555E-01	5.54870037158E-01	4.31516815406E+03	8.90769041465E-01	3.79823919289E-01
3.48756097555E-01	5.70301266654E-01	4.46077086836E+03	9.01338799553E-01	3.85809059769E-01
3.47756097555E-01	5.86318136603E-01	4.61276304651E+03	9.12162408758E-01	3.91937943804E-01
3.46756097555E-01	6.02949937221E-01	4.77148838835E+03	9.23249125247E-01	3.98215812711E-01
3.45756097555E-01	6.20227795639E-01	4.93731305447E+03	9.34608660731E-01	4.04648165759E-01
3.44756097555E-01	6.38184815245E-01	5.11062741548E+03	9.46251210843E-01	4.11240776242E-01
3.43756097555E-01	6.56856227493E-01	5.29184796046E+03	9.58187485657E-01	4.17999708752E-01
3.42756097555E-01	6.76279557448E-01	5.48141938138E+03	9.70428742551E-01	4.24931337798E-01
3.41756097555E-01	6.96494804521E-01	5.67981685211E+03	9.82986821620E-01	4.32042367848E-01
3.40756097555E-01	7.17544639990E-01	5.88754852295E+03	9.95874183870E-01	4.39339854966E-01
3.39756097555E-01	7.39474623126E-01	6.10515825401E+03	1.00910395247E+00	4.46831230162E-01
3.38756097555E-01	7.62333437936E-01	6.33322861398E+03	1.02268995731E+00	4.54524324635E-01
3.37756097555E-01	7.86173152808E-01	6.57238417382E+03	1.03664678324E+00	4.62427397078E-01
3.36756097555E-01	8.11049505615E-01	6.82329512879E+03	1.05098982230E+00	4.70549163253E-01
3.35756097555E-01	8.37022217175E-01	7.08668128660E+03	1.06573533034E+00	4.78898828053E-01
3.34756097555E-01	8.64155336322E-01	7.36331646432E+03	1.08090048847E+00	4.87486120309E-01
3.33756097555E-01	8.92517620289E-01	7.6540334225E+03	1.09650346983E+00	4.96321330597E-01
3.32756097555E-01	9.22182954577E-01	7.95972882970E+03	1.11256351231E+00	5.05415352382E-01
3.31756097555E-01	9.53230817065E-01	8.28137000483E+03	1.12910099757E+00	5.14779726825E-01
3.30756097555E-01	9.85746791771E-01	8.62000069943E+03	1.14613753745E+00	5.24426691646E-01

Printed in the United States of America
Available from
National Technical Information Service
U.S. Department of Commerce
5285 Port Royal Road
Springfield, VA 22161

Microfiche (A01)

NTIS Page Range	Price Code	NTIS Page Range	Price Code
001-025	A02	131-175	A08
026-050	A03	176-200	A09
051-075	A04	201-225	A10
076-100	A05	226-250	A11
101-125	A06	251-275	A12
126-150	A07	276-300	A13

*Contact NTIS for a price quote.

NTIS Page Range	Price Code	NTIS Page Range	Price Code
301-325	A14	451-475	A20
326-350	A15	476-500	A21
351-375	A16	501-525	A22
376-400	A17	526-550	A23
401-425	A18	551-575	A24
426-450	A19	576-600	A25
501 up*		A29	

LOS ALAMOS
NATIONAL LABORATORY

MAR 16 1973.

RECEIVED

Los Alamos Los Alamos National Laboratory
New Mexico 87545